Title:

# Scleral Topography analysed by Optical Coherence Tomography

Authors:

Stefan Bandlitz,[1,2] Joachim Bäumer,[1] Uwe Conrad[1], James Wolffsohn[2]

[1]Höhere Fachschule für Augenoptik Köln (Cologne School of Optometry), Cologne, Germany

[2]Ophthalmic Research Group, Life and Health Sciences, Aston University, Birmingham, UK

Tables and Figures: 1 Table and 7 Figures

Word count: 3011

Corresponding Author

Stefan Bandlitz

Höhere Fachschule für Augenoptik Köln

(Cologne School of Optometry)

Bayenthalgürtel 6-8

D-50968 Köln, Germany

e-mail: bandlitz@hfak.de

Telephone: 0049-221-348080

**ABSTRACT**

**Purpose:** A detailed evaluation of the corneo-scleral-profile (CSP) is of particular relevance in soft and scleral lenses fitting. The aim of this study was to use optical coherence tomography (OCT) to analyse the profile of the limbal sclera and to evaluate the relationship between central corneal radii, corneal eccentricity and scleral radii.

**Methods:** Using OCT (Optos OCT/SLO; Dunfermline, Scotland, UK) the limbal scleral radii (SR) of 30 subjects (11M, 19F; mean age 23.8 ±2.0SD years) were measured in eight meridians 45º apart. Central corneal radii (CR) and corneal eccentricity (CE) were evaluated using the Oculus Keratograph 4 (Oculus, Wetzlar, Germany). Differences between SR in the meridians and the associations between SR and corneal topography were assessed.

**Results:** Median SR measured along 45° (58.0; interquartile range, 46.8-84.8mm) was significantly ($p<0.001$) flatter than along 0° (30.7; 24.5-44.3mm), 135° (28.4; 24.9-30.9mm), 180° (23.40; 21.3-25.4mm), 225° (25.8; 22.4-32.4mm), 270° (28.8; 25.3-33.1mm), 315° (30.0; 25.0-36.9mm), and 90° (37.1; 29.1-43.4mm). In addition, the nasal SR along 0° were significant flatter than the temporal SR along 180° ($p<0.001$). Central corneal radius in the flat meridian (7.83±0.26mm) and in the steep meridian (7.65±0.26mm) did not correlate with SR ($p=0.186$ to 0.998). There was no statistically significant correlation between corneal eccentricity and scleral radii in each meridian ($p=0.422$).

**Conclusions:** With the OCT device used in this study it was possible to measure scleral radii in eight different meridians. Scleral radii are independent of corneal topography and may provide additional data useful in fitting soft and scleral contact lenses.

**Key words:** Scleral radius, optical coherence tomography, cornea radius, corneal eccentricity, corneo-scleral topography.

The selection of the back-surface design of rigid contact lenses was traditionally based on the topography of the central cornea measured by a keratometer. More advanced procedures such as placido-based corneal topography and Scheimpflug tomography allow a more detailed description of the anterior shape of the central, para-central and peripheral cornea. While the topography of the cornea is essential in selecting and predicting the fit of a rigid contact lens [1-3], a weak or no correlation was found between corneal topography and soft contact lens fit [4, 5]. Furthermore, modern rigid scleral contact lenses have gained renewed interest during the last decade and becoming more widely used [6, 7]. Therefore, a precise analysis of the topography of the limbal sclera and the cornea-scleral transition zone is of increasing interest in the fitting process of rigid scleral contact lenses [8, 9], and seems to be a more reliable method to predict the fitting of a soft contact lens [4, 10-12].

Formerly, the topography of the limbal and anterior scleral shape only could be analyzed by the use of an invasive imprint technique [13, 14], where a mould is made of the anterior surface and then used as a positive cast to produce a scleral lens [6], or by grading the limbal profiles termed “Corneo-Scleral-Profile (CSP)” at the slit-lamp [15-18]. The CSP is the profile-line that is formed by the shape of the cornea, the sulcus and the sclera. It was first mentioned by Gaggioni and Meier [16], who classified the profile in five different shapes. In clinical practice the CSP can be evaluated by the help of a slit-lamp or a magnifier. However, Bokern et al. [17] reported a low accuracy and repeatability of this subjective grading method.

The Eye Surface Profiler (ESP) is a newly developed cornea and sclera topographer that can measure up to 20 mm width of the anterior surface of the eye. The technology is based on Fourier transform profilometry which involves projecting and imaging placido discs from two oblique angles onto the cornea consecutively, integrating the results; a prototype of the instrument was first developed by Jongsma et al. [19]. To achieve good results with the ESP it needs to be considered that the instillation of fluorescein is required and that the alignment procedure differs from placido-based systems [20]. However, in a recently published study it was shown that the ESP can be used to calculate the scleral radius with high precision [9] .

Optical coherence tomography (OCT) provides non-invasive high-resolution images of most ocular tissues. While the initial focus was on imaging the posterior segment of the eye, there are now a number of commercial instruments on the market which in addition allow imaging and measurements on the anterior segment of the eye [21-23]. Beside the measurement of the corneal topography from limbus to limbus [22], OCT has already been applied to describe the radii of the sclera [11, 12, 24]. However, in previous studies the description of the scleral shape was limited to two or four quadrants. Furthermore, it remains unknown whether the topography of the scleral is related to the topography of the cornea.

Consequently, the aims of this study were to analyse the profile of the limbal region sclera over 8 meridians of the ocular surface and to evaluate any relationship between central corneal radii, corneal eccentricity and scleral radii.

## MATERIALS AND METHODS

### *Subjects*

Thirty healthy subjects (mean age 23.8 ± 2.0 (SD) years, male = 11, female = 19) were recruited from the students of the Höhere Fachschule für Augenoptik Köln (Cologne School of Optometry), Cologne, Germany.

Subjects were excluded if they had a current or previous condition known to affect the conjunctiva or the sclera such as pterygium and pinguecula; had a history of previous ocular surgery, including refractive or strabismus surgery, eyelid surgery, or corneal surgery; had any previous ocular trauma, were diabetic, were taking medication known to affect the ocular surface or sclera, and/or had worn rigid contact lenses or soft contact lenses during the preceding 24 hours prior to the study. The study was approved by the Research Ethics Committee and all subjects gave written informed consent before participating in the study. The procedures were conducted in accordance with the requirements of the Declaration of Helsinki (1983) and patient data were used only in anonymized form.

### *Instruments*

The images of the sclera were obtained using an Optos OCT/SLO™ (Optos plc, Dunfermline, Scotland, UK) (Figure 1). This instrument combines spectral domain OCT imaging (SD-OCT) with a confocal scanning laser ophthalmoscope (SLO) in one instrument. The add-on lens was placed in front of the optics to focus the system on the anterior segment of the eye. To enable the measurement of the scleral radii in different orientations, a black board with white fixation crosses in 0° (nasal), 45° (superonasal), 90° (superior), 135° (superotemporal), 180° (temporal), 225°

(inferotemporal), 270° (inferior) and in 315° (inferonasal) was designed and fixed to the instrument (Figure 1). Since the measurement in the different orientation is dependent upon the subject initial alignment, head and chin rest were adjusted while the patient was fixating the central target of the instrument. Central alignment was controlled before each peripheral measurement.

Central corneal radii for the flat ($r_{c/fl}$) and steep ($r_{c/st}$) meridian as well as corneal eccentricity for the nasal ($e_{nas}$), temporal ($e_{temp}$), inferior ($e_{inf}$) and superior ($e_{sup}$) direction were measured using a topograph (Keratograph 4; Oculus Optikgeräte GmbH, Wetzlar, Germany).

***Sample calibration***

To ensure that on-screen images of the OCT represented curvature of known dimensions, the outer surface of three optical precision glass beads (radius 20, 22 and 28 mm; Hilgenberg GmbH, Malsfeld, Germany) were used as a model for the sclera. The outer diameters of the glass capillaries were confirmed by use of a gauge. Three OCT scans were taken for each glass bead. The OCT images were than exported to ImageJ software (http://imagej.nih.gov/ij/) and a circle was fitted to the confirmed radius of the glass beads. A regression line was then calculated to form a calibration curve, which was used to correct the OCT measurements of the sclera. The OCT measurements of the glass beads were compared at two different sessions at the same time of day. Repeated measurements between day 1 and day 2 were not significantly different (paired t-test; p=0.447). The 95% confidence intervals around differences indicate good repeatability (95% CI: -1.69 to +1.46mm) of the method *in vitro.*

***Procedures***

OCT images and topograph measurements were taken during one study visit in a randomized order. One operator collected data from the right eye only.

For the recording the OCT images, subjects were asked to look at the fixation targets along 0, 45, 90, 135, 180, 225, 270 and 315 degrees, in a randomized order. The SLO image of the OCT was used to find the correct position for a line scan (Figure 2). To set up and to check the correct position of the sclera to be measured and to ensure a constant alignment of the OCT, a millimetre grid was attached on the computer screen. The OCT scan axis was moved forwards and backwards until the apex of the sclera was in congruence with a marked horizontal line on the screen, and it was moved left and right until the scleral spur was in congruence with a vertical line on the screen (Figure 3). The OCT images were saved as JPEGs, for subsequent analysis with ImageJ 1.46 software (http://rsbweb.nih.gov/ij). In ImageJ the three-point circle fit technique was applied to calculate the radius of the sclera at the different locations (Figure 4). The mean of three consecutive measurements of the scleral-radii in the different meridians was recorded. Repeated measurements of 11 subjects between day 1 and day 2 were not significantly different (Wilcoxon signed-rank test; p=0.501). The 95% confidence intervals around differences indicate good repeatability (95% CI: -0.43 to +1.57mm) of the method *in vivo.*

Topography measurements of the central corneal radii and corneal eccentricity were obtained while the subject was looking straight ahead with the left eye occluded. The mean of three consecutive measurements of central radii and corneal was calculated.

**Statistical methods**

Data were tested for normality using the Shapiro-Wilk test. As scleral radii were not normally distributed differences between the scleral radii in the different sectors were analysed by Friedman Test followed by Bonferroni correction. Correlation between central corneal radii and scleral radii as well as between corneal eccentricity and scleral radii were analysed using the Spearman's Rank correlation coefficient. The data were analysed using SigmaPlot 12 (Systat Software Inc., Chicago, USA).

## RESULTS

The mean values ± standard deviations, the median and the minimum and maximum values of central corneal radii and corneal eccentricity, are summarised in Table 1.

The median superonasal (45°) scleral radius (58.0; interquartile range, 46.8-84.8mm) was significantly ($p<0.001$) flatter than the radii measured nasal (30.7; 24.5-44.3mm), superotemporal (28.4; 24.9-30.9mm), temporal (23.40; 21.3-25.4mm), inferotemporal (25.8; 22.4-32.4mm), inferior (28.8; 25.3-33.1mm), inferonasal (30.0; 25.0-36.9mm), and superior (37.1; 29.1-43.4mm) (Figure 5 and 6). Scleral radius measured superiorly was significantly flatter than the radii measured temporal ($p=0.015$). Nasal scleral radius was significantly flatter than temporal radius ($p<0.001$). There was no statistically significant difference between the scleral radii measured in the other directions ($p>0.05$).

There was no statically significant correlation between central corneal radii and scleral radii (p = 0.186 to 0.998) and no significant correlation between the mean corneal eccentricity and the mean scleral radius (p = 0.422).

## DISCUSSION

This study reports the use of a spectral domain OCT combined with a confocal scanning laser ophthalmoscope to evaluate the radius and therefore the profile of the limbal sclera in eight meridians. Using this instrument, differences between scleral radii at the different locations were found, with the flattest scleral radius in the superonasal and the steepest radius in the temporal limbal region.

Hall et al. [11, 12] used a time–domain anterior segment optical coherence tomographer in 204 subjects to measure the scleral radius in four quadrants. They found scleral radii to be nasal 35.5±39.4 mm, temporal 22.4±12.7mm, superior 29.3±17.4mm and inferior 33.5±29.6mm, which is in good agreement with the results of this study. Furthermore, like in this study the reported scleral curvature was steepest in the temporal sclera. Likewise, Choi et al. [25] also using time-domain OCT reported that the mean radius of nasal anterior scleral curvature was significantly greater than that of temporal anterior scleral curvature (the only two meridians assessed). However, the reported radii for nasal anterior scleral (13.33±1.12mm) and temporal anterior scleral (12.32±0.77mm) were much steeper than the results of this study and the two studies presented by Hall et al. [11, 12]. This might be explained by the fact that Choi and colleagues calculated the axial (sagittal) radius of the sclera while in the studies of Hall et al. [11, 12] and in this study the tangential scleral radius was assessed. As the tangential radius requires no assumption concerning the location of the optic axis, the tangential radius gives a truer picture of off-axis irregularities than the sagittal radius [26-28]; hence the tangential radius seems to be more useful then the sagittal measurement in the detection of topographic abnormalities and surface shape changes, as in accurate GP base curve selection [28-32].

Nevertheless, manufacturers of both soft and scleral contact lenses and clinicians are widely used to working with axial or sagittal radii. In corneal topography the sagittal radius can be calculated from a given tangential radius if additional information like the central corneal radius, the fixation angle and the distance from corneal apex is given [33]. The measuring of the tangential scleral radius with OCT is based on a single peripheral cross section. To derive an axial scleral radius from a given tangential scleral radius several assumptions and a manual assembly of different OCT images into one single circular image are required [25]. Applying this technique the scleral is assumed to be rotationally symmetric and therefore the results of scleral shape might be spherically biased [25, 34].

Applying Scheimpflug photography for the measurement of scleral curvature, Tiffany et al. [35] reported scleral radii from 13.3 to 14.3 mm for the temporal scleral close to the limbus, wherein the exact measuring location was not described.  Jesus et al. [9] used the newly developed ESP to measure the scleral radius of the naso-temporal area and reported values of 11.2±0.3 mm. To differentiate the scleral topography from the cornea topography a circular band between 5 and 6.5 mm from corneal apex was removed from the analysis in their study. In contrast in this study, the radius was measured in a 3 mm zone starting from scleral spur and might include parts of the limbal region. Therefore, it is likely that different parts of the sclera were analysed which might explain the differences in measured radii.

In this study scleral radii additionally were measured in the oblique meridians, indicating the flattest radii was along 45° (superonasal), albeit a huge range was found (Table 1) (Figure 6 and 7). Kasahara at al. [36] determined the differences in scleral shape between the superonasal and superotemporal quadrants using a swept source OCT. They showed that the scleral curvature in the superonasal quadrant (34.3±12.6mm) was significantly flatter than that in the superotemporal quadrant (18.3±3.6mm), which is in concordance the findings of this study. While they were measuring over a radius of 5 mm, in the present study about 3 mm radius were analysed which might explain the smaller values they reported.

Using an anterior segment time-domain OCT, the Pacific University studies measured the limbal and scleral angles in reference to the horizontal plane [6]. They found the smallest angles in the superonasal region of the sclera and the largest angle in the temporal region, which seems to correspond with the flattest radii for the superonasal and the steepest radii for the temporal region measured in this study.

Interestingly, in a recently published study by Ebneter et al. [37] mean scleral thickness was also found to significantly different between quadrants. Applying a spectral domain OCT, they investigated the sclera scleral thickness in the inferonasal, inferotemporal, superotemporal, and superonasal quadrant, 2 mm from the scleral spur. The sclera was found to be thinnest in the superonasal region where in this study the flattest scleral radius was found. So it might be hypothesized that variations in scleral thickness influences the curvature of the scleral in the limbal region. Scleral thickness seems to increase with age and was found to be variable in a 2.5 mm zone form scleral spur [37, 38]. Furthermore, it was shown that scleral radii negatively correlate with age [12]. From this it might be postulate that a thick limbal sclera results in steeper scleral radii, while a thin sclera result in flatter scleral radii. Therefore, it is likely that age related changes as well as variations in scleral thickness influence scleral radii resulting in a non-spherical shape of the limbal scleral region as it was found in this study.

From the literature it is known that central keratometry is a poor predictor of soft contact lens fit and the addition of videokeratoscopy at best slightly improved the prediction, while topography of the limbal region sclera seems to be a more reliable method to predict the fitting of soft contact lenses [4, 5, 11]. This seems to be consistent with the findings of this study since the topography of the cornea was not related to the topography of the limbal region scleral. Moreover, the topographer used in this study was not able to describe the corneal shape from limbus to limbus, although an 8 mm diameter area could be achieved.

Applying the OCT technique to measure scleral radii has some limitations. For the measurement of scleral radii in different orientations it is required that the patient had to fixate several paracentral target. While fixating, the tonus of the ocular muscles may have had an influence on the scleral profile. However, this also reflects the dynamic eye movements a contact lens wearer will make while wearing their lenses. Furthermore, this method is dependent on a correct and repeatable alignment of the system as well as on the manual fitting of a circle in external software. Therefore, the operator dependency of the OCT measurement of scleral radii needs to be addressed in further studies.

In summary, with the spectral domain OCT used in this study it was possible to measure scleral radii along eight different meridians. Scleral radii were found to be independent of corneal topography and may provide additional data useful in fitting soft and scleral contact lenses.

**Conflict of interest**

None

**REFERENCES**

[1] Szczotka LB, Capretta DM, Lass JH. Clinical evaluation of a computerized topography software method for fitting rigid gas permeable contact lenses. CLAO J. 1994;20:231-6.

[2] Jani BR, Szczotka LB. Efficiency and accuracy of two computerized topography software systems for fitting rigid gas permeable contact lenses. CLAO J. 2000;26:91-6.

[3] Cosar CB, Sener AB. Orbscan corneal topography system in evaluating the anterior structures of the human eye. Cornea. 2003;22:118-21.

[4] Young G, Schnider C, Hunt C, Efron S. Corneal topography and soft contact lens fit. Optom Vis Sci. 2010;87:358-66.

[5] Szczotka LB, Roberts C, Herderick EE, Mahmoud A. Quantitative descriptors of corneal topography that influence soft toric contact lens fitting. Cornea. 2002;21:249-55.

[6] van der Worp E, Bornman D, Ferreira DL, Faria-Ribeiro M, Garcia-Porta N, Gonzalez-Meijome JM. Modern scleral contact lenses: A review. Cont Lens Anterior Eye. 2014;37:240-50.

[7] Schornack MM. Scleral lenses: a literature review. Eye Contact Lens. 2015;41:3-11.

[8] Gemoules G. A novel method of fitting scleral lenses using high resolution optical coherence tomography. Eye Contact Lens. 2008;34:80-3.

[9] Jesus DA, Kedzia R, Iskander DR. Precise measurement of scleral radius using anterior eye profilometry. Cont Lens Anterior Eye. 2017;40:47-52.

[10] Wolffsohn JS, Drew T, Dhallu S, Sheppard A, Hofmann GJ, Prince M. Impact of soft contact lens edge design and midperipheral lens shape on the epithelium and its indentation with lens mobility. Invest Ophthalmol Vis Sci. 2013;54:6190-7.

[11] Hall LA, Young G, Wolffsohn JS, Riley C. The influence of corneoscleral topography on soft contact lens fit. Invest Ophthalmol Vis Sci. 2011;52:6801-6.

[12] Hall LA, Hunt C, Young G, Wolffsohn J. Factors affecting corneoscleral topography. Invest Ophthalmol Vis Sci. 2013;54:3691-701.

[13] Lyons CJ, Buckley RJ, Pullum K, Sapp N. Development of the gas-permeable impression-moulded scleral contact lens. A preliminary report. Acta ophthalmologica Supplement. 1989;192:162-4.

[14] Pullum K, Buckley R. Therapeutic and ocular surface indications for scleral contact lenses. Ocul Surf. 2007;5:40-8.

[15] Meier D. Das Corneo-Skleral-Profil ein Kriterium individueller Kontaktlinsenanpassung. Die Kontaktlinse. 1992;26:4-11.

[16] Gaggioni M, Meier D. Das Corneo-Skleral-Profil. NOJ. 1987;1:66-71.

[17] Bokern S, Hoppe M, Bandlitz S. Genauigkeit und Wiederholbarkeit bei der Klassifizierung des Corneo-Skleral-Profils. Die Kontaktlinse. 2007;40:26-8.

[18] Marriott PJ. An analysis of the global contours and haptic contact lens fitting. The British journal of physiological optics. 1966;23:1-40.

[19] Jongsma FH, de Brabander J, Hendrikse F, Stultiens BA. Development of a wide field height eye topographer: validation on models of the anterior eye surface. Optom Vis Sci. 1998;75:69-77.

[20] Iskander DR, Wachel P, Simpson PN, Consejo A, Jesus DA. Principles of operation, accuracy and precision of an Eye Surface Profiler. Ophthalmic Physiol Opt. 2016;36:266-78.

[21] Wojtkowski M, Kaluzny B, Zawadzki RJ. New directions in ophthalmic optical coherence tomography. Optom Vis Sci. 2012;89:524-42.

[22] Ortiz S, Siedlecki D, Perez-Merino P, Chia N, de Castro A, Szkulmowski M, et al. Corneal topography from spectral optical coherence tomography (sOCT). Biomedical optics express. 2011;2:3232-47.

[23] Lim SH. Clinical applications of anterior segment optical coherence tomography. Journal of ophthalmology. 2015;2015:605729.

[24] Tan B, Graham AD, Tsechpenakis G, Lin MC. A novel analytical method using OCT to describe the corneoscleral junction. Optom Vis Sci. 2014;91:650-7.

[25] Choi HJ, Lee SM, Lee JY, Lee SY, Kim MK, Wee WR. Measurement of anterior scleral curvature using anterior segment OCT. Optom Vis Sci. 2014;91:793-802.

[26] Salmon TO, Horner DG. Comparison of elevation, curvature, and power descriptors for corneal topographic mapping. Optometry and vision science : official publication of the American Academy of Optometry. 1995;72:800-8.

[27] Chan JS, Mandell RB, Burger DS, Fusaro RE. Accuracy of videokeratography for instantaneous radius in keratoconus. Optometry and vision science : official publication of the American Academy of Optometry. 1995;72:793-9.

[28] Ying J, Wang B, Shi M. Anterior corneal asphericity calculated by the tangential radius of curvature. Journal of biomedical optics. 2012;17:075005.

[29] Gemoules G. Comparison of axial and tangential topographic algorithms for contact lens fitting after LASIK. Eye & contact lens. 2006;32:158-9; author reply 9.

[30] Rabinowitz YS. Tangential vs sagittal videokeratographs in the "early" detection of keratoconus. Am J Ophthalmol. 1996;122:887-9.

[31] Szczotka-Flynn L, Jani BR. Comparison of axial and tangential topographic algorithms for contact lens fitting after LASIK. Eye & contact lens. 2005;31:257-62.

[32] Tummanapalli SS, Potluri H, Vaddavalli PK, Sangwan VS. Efficacy of axial and tangential corneal topography maps in detecting subclinical keratoconus. Journal of cataract and refractive surgery. 2015;41:2205-14.

[33] Bennett AG, Rabbetts RB. What radius does the conventional keratometer measure? Ophthalmic Physiol Opt. 1991;11:239-47.

[34] Ying J, Cai J, Zhu L, Zha Y. Comprehensive Evaluation of Anterior Corneal Change in Asphericity Calculated by the Tangential Radius of Curvature after LASIK. Journal of ophthalmology. 2017;2017:3874371.

[35] J.M. Tiffany, E.F. Grande, B.S. Todd. Measurement of scleral curvature by scheimpflug photography. Invest Ophthalmol. 2004;45:2389.

[36] Kasahara M, Shoji N, Morita T, Shimizu K. Comparative optical coherence tomography study of differences in scleral shape between the superonasal and superotemporal quadrants. Jpn J Ophthalmol. 2014;58:396-401.

[37] Ebneter A, Haner NU, Zinkernagel MS. Metrics of the normal anterior sclera: imaging with optical coherence tomography. Graefes Arch Clin Exp Ophthalmol. 2015;253:1575-80.

[38] Read SA, Alonso-Caneiro D, Free KA, Labuc-Spoors E, Leigh JK, Quirk CJ, et al. Diurnal variation of anterior scleral and conjunctival thickness. Ophthalmic Physiol Opt. 2016;36:279-89.

**Figures**

**Figure 1.** Optos spectral domain OCT/SLO™ (Optos plc, Dunfermline, Scotland, UK) with a custom made black board and white fixation crosses in the eight different meridians.

**Figure 2.** Image of the confocal scanning laser ophthalmoscope (SLO) (left) and OCT image (right) of a line scan in an oblique position.

**Figure 3.** Millimetre grid attached on the computer screen to check the correct position of the sclera to be measured and to ensure a constant alignment of the OCT. Apex of the sclera in congruence with a marked horizontal line (arrow 1) and scleral spur in congruence with a vertical line on the screen (arrow 2).

**Figure 4.** ImageJ 1.46 software (http://rsbweb.nih.gov/ij) for curve fitting and analysis of scleral radius on OCT image.

**Figure 5.** Median values of scleral radii in the eight meridians. Red colour is marking the steepest while blue colour is marking the flattest meridian found in this study.

**Figure 6.** Box plot showing the scleral radii in the different meridians. (Upper horizontal line of box, 75th percentile; lower horizontal line of box, 25th percentile; horizontal bar within box, median; upper horizontal bar outside box, 95th percentile; lower horizontal bar outside box, 5th percentile. Circles represent outliers.)

**Figure 7.** Examples of OCT images taken from a steep (upper image) and a flat (lower image) scleral radius.

## Tables

**Table 1.** Mean values ± standard deviations, the median and the minimum and maximum values of scleral radii (measured on OCT Images), central corneal radii and corneal eccentricity (measured with topography).

**Table 1**

| | Mean ± SD | Median | Range |
|---|---|---|---|
| **Scleral radius [mm]** | | | |
| Nasal (0°) | 35.29 ± 17.68 | 30.73 | 18.52 – 110.11 |
| Superonasal (45°) | 74.57 ± 45.97 | 58.00 | 24.88 – 237.18 |
| Superior (90°) | 45.00 ± 31.99 | 37.11 | 17.55 – 181.78 |
| Superotemporal (135°) | 29.41 ± 7.70 | 28.36 | 21.75 – 60.76 |
| Temporal (180°) | 24.40 ± 4.86 | 23.36 | 17.34 – 36.21 |
| Inferotemporal (225°) | 27.17 ± 5.90 | 25.76 | 19.29 – 42.91 |
| Inferior (270°) | 31.42 ± 13.44 | 28.75 | 20.44 – 95.90 |
| Inferonasal (315°) | 36.46 ± 34.64 | 29.96 | 16.70 – 213.76 |
| | **37.97 ± 12.77** | **32.75** | |
| **Central corneal radius [mm]** | | | |
| Flat meridian | 7.83 ± 0.26 | 7.75 | 7.38 – 8.45 |
| Steep meridian | 7.65 ± 0.26 | 7.57 | 7.26 – 8.29 |
| | **7.74 ± 0.26** | **7.66** | |
| **Corneal eccentricity** | | | |
| Nasal | 0.60 ± 0.18 | 0.62 | -0.09 – 0.86 |
| Superior | 0.46 ± 0.18 | 0.51 | -0.19 – 0.79 |
| Temporal | 0.47 ± 0.08 | 0.46 | 0.29 – 0.67 |
| Inferior | 0.42 ± 0.27 | 0.46 | -0.49 – 0.92 |
| | **0.49 ± 0.12** | **0.49** | |

Figure 1

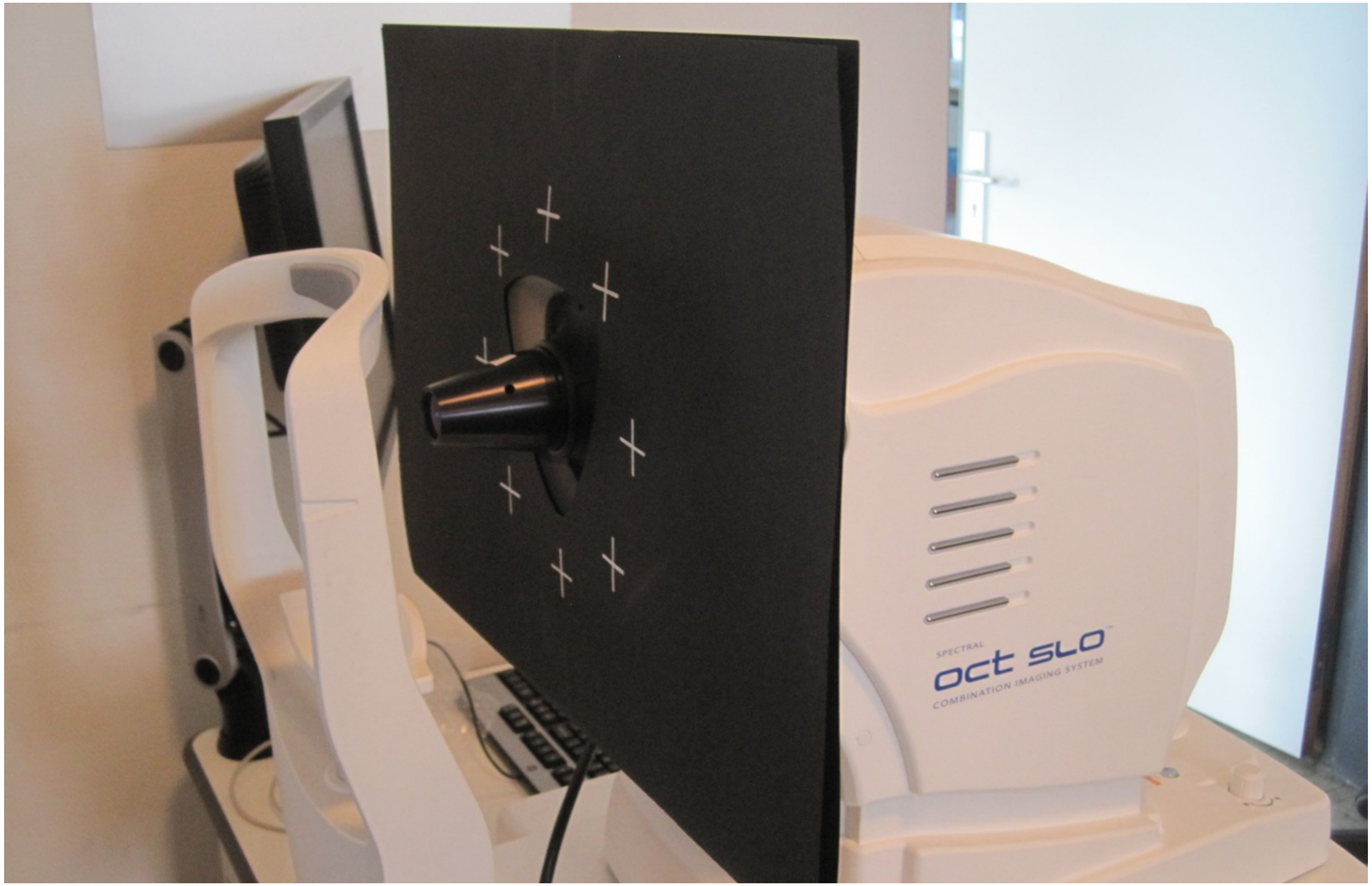

**Figure 2**

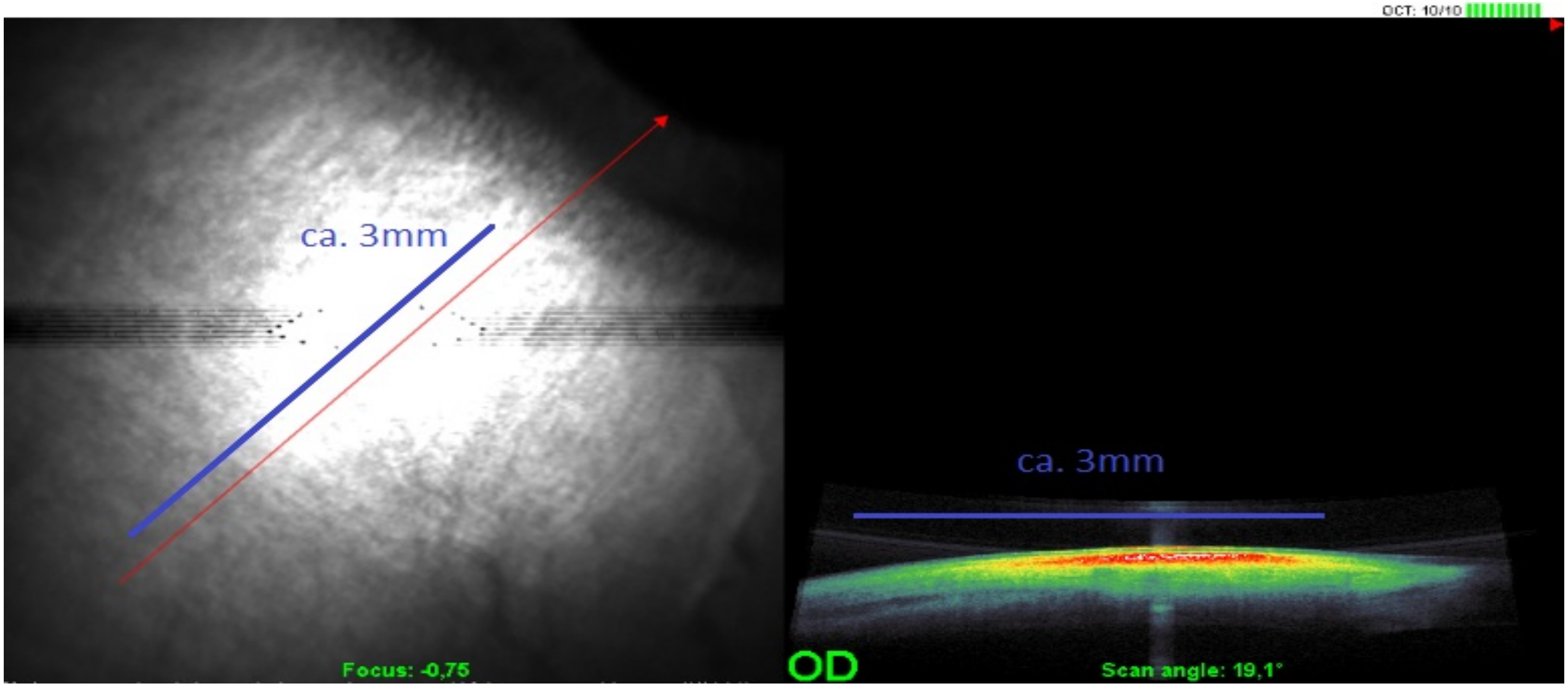

**Figure 3**

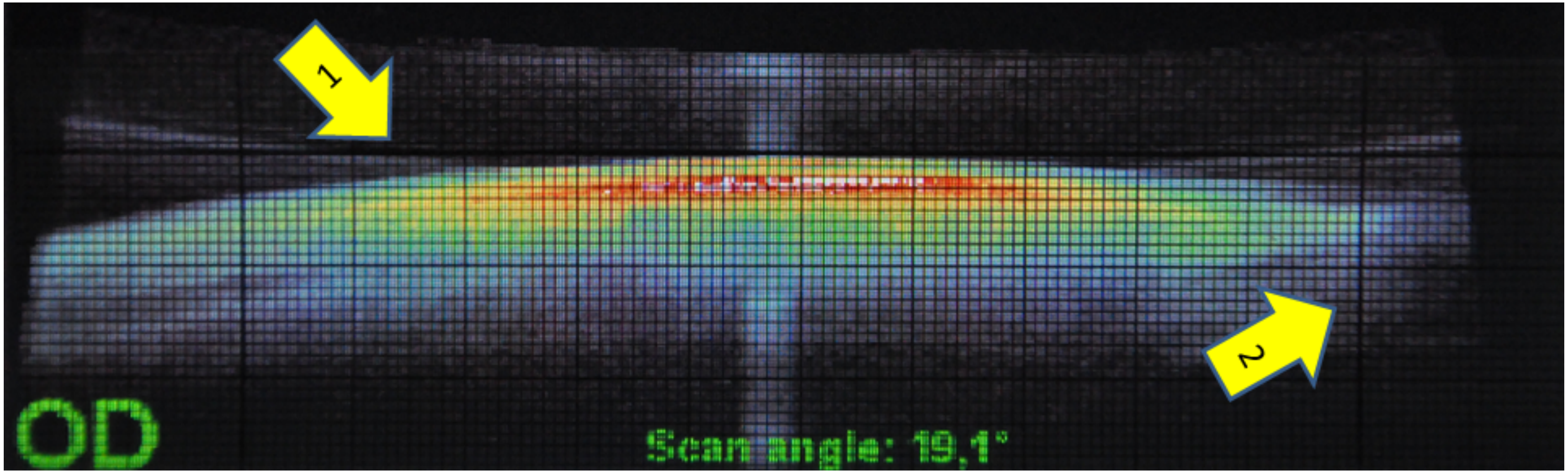

**Figure 4**

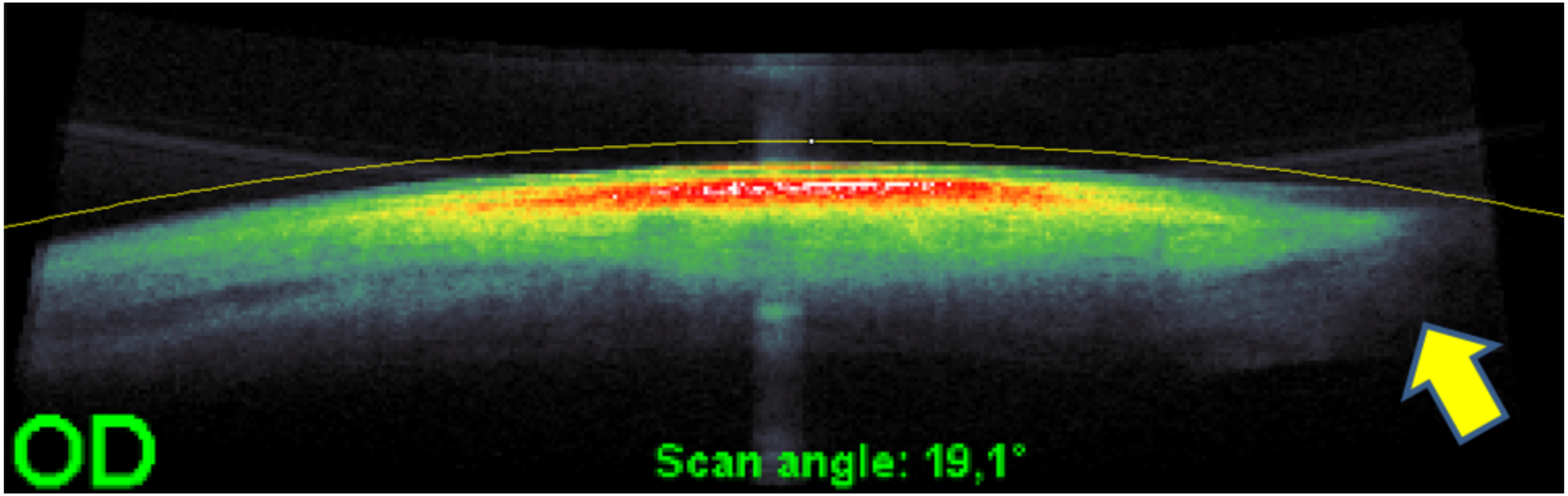

Figure 5

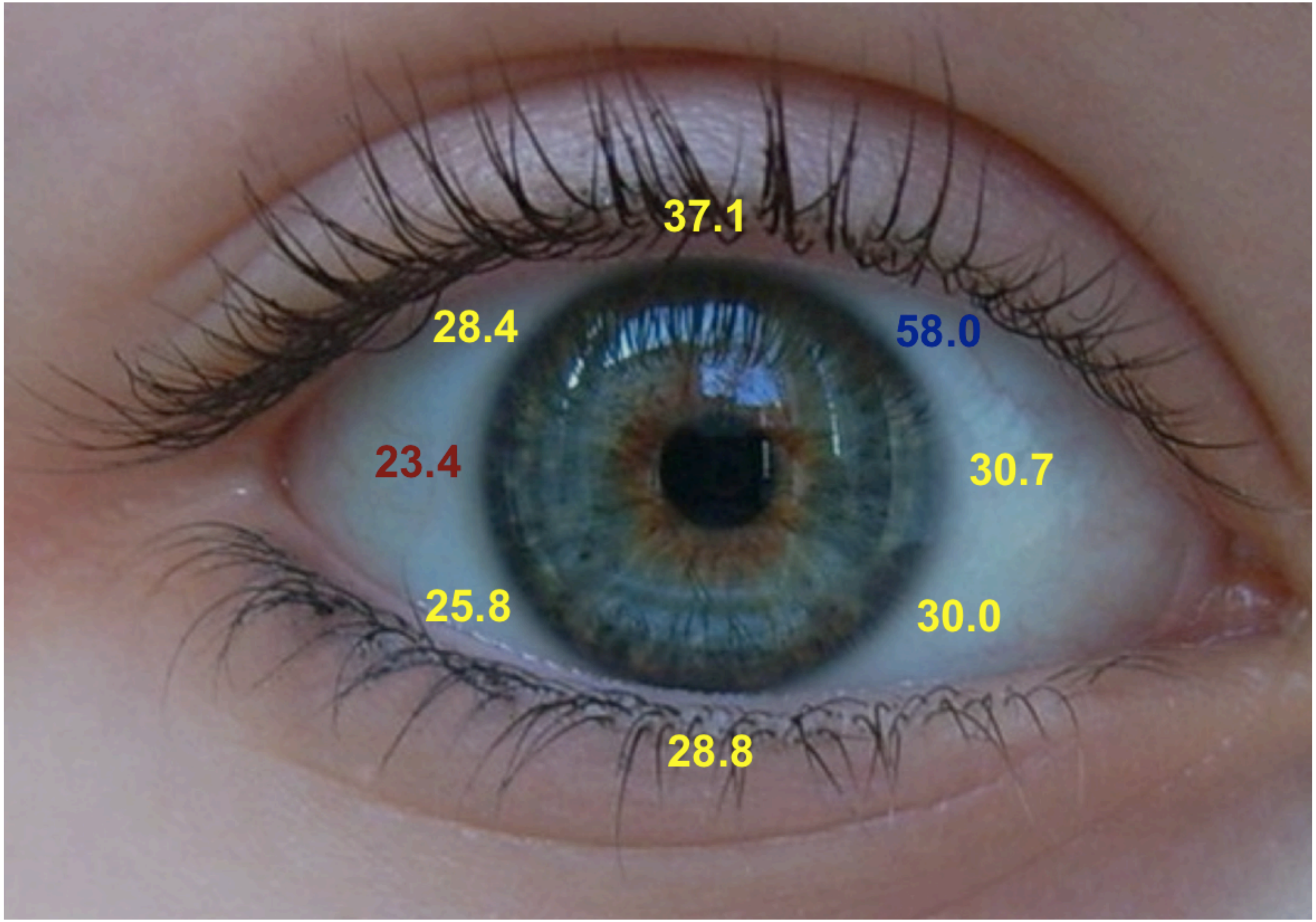

Figure 6

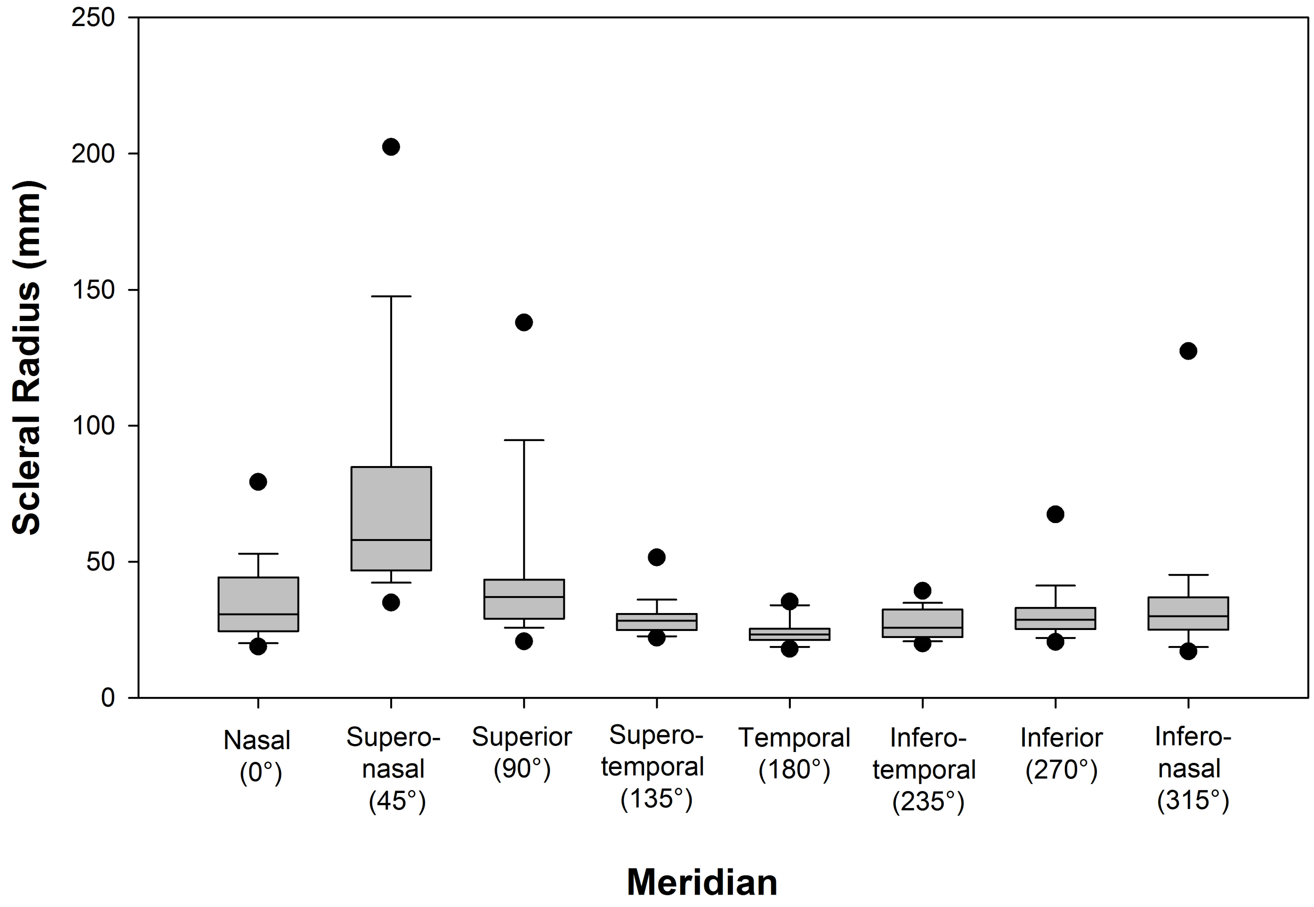
Scleral Radius (mm)
250
200
150
100
50
0
Nasal (0°)
Supero-nasal (45°)
Superior (90°)
Supero-temporal (135°)
Temporal (180°)
Infero-temporal (235°)
Inferior (270°)
Infero-nasal (315°)
Meridian

**Figure 7**

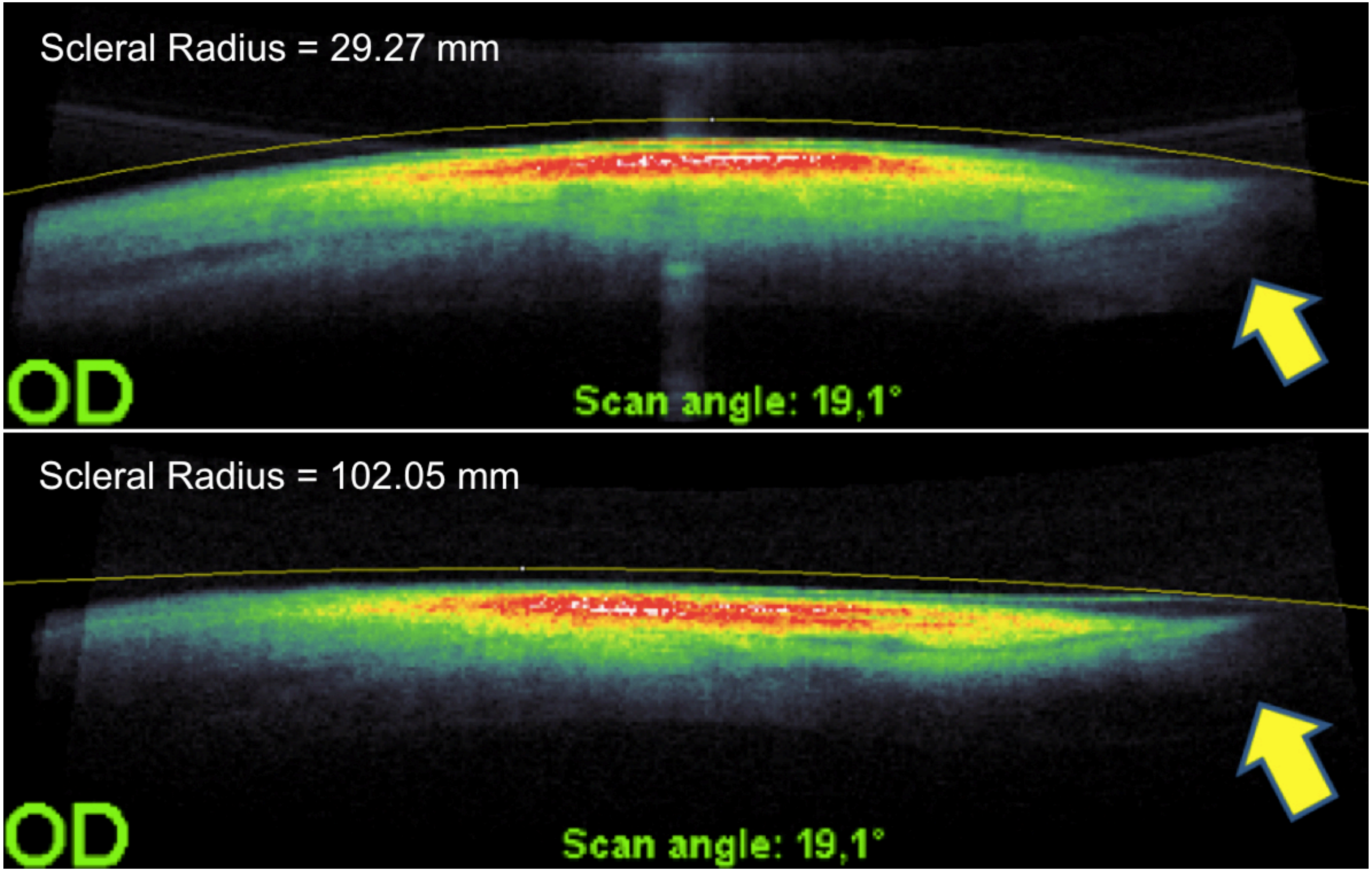
Scleral Radius = 29.27 mm
OD
Scan angle: 19,1°
Scleral Radius = 102.05 mm
OD
Scan angle: 19,1°